Extrapore Residues of the S5-S6 Loop of Domain 2 of the Voltage-Gated Skeletal Muscle Sodium Channel (rSkM1) Contribute to the μ-Conotoxin GIIIA Binding Site

M. Chahine,* J. Sirois,* P. Marcotte,* L.-Q. Chen,# and R. G. Kallen#§

*Laval Hospital, Research Center, Ste.-Foy, Québec, G1V 4G5 Canada, and #Department of Biochemistry and Biophysics and §Mahoney Institute of Neurological Sciences, University of Pennsylvania School of Medicine, Philadelphia, Pennsylvania 19104 USA

ABSTRACT The tetradomain voltage-gated sodium channels from rat skeletal muscle (rSkM1) and from human heart (hH1) possess different sensitivities to the 22-amino-acid peptide toxin, μ-conotoxin GIIIA (μ-CTX). rSkM1 is sensitive (IC_{50} = 51.4 nM) whereas hH1 is relatively resistant (IC_{50} = 5700 nM) to the action of the toxin, a difference in sensitivity of >100-fold. The affinity of the μ-CTX for a chimera formed from domain 1 (D1), D2, and D3 from rSkM1and D4 from hH1 (SSSH; S indicates origin of domain is skeletal muscle and H indicates origin of domain is heart) was paradoxically increased approximately fourfold relative to that of rSkM1. The source of D3 is unimportant regarding the difference in the relative affinity of rSkM1 and hH1 for μ-CTX. Binding of μ-CTX to HSSS was substantially decreased (IC_{50} = 1145 nM). Another chimera with a major portion of D2 deriving form hH1 showed no detectable binding of μ-CTX (IC_{50} > 10 μM). These data indicate that D1 and, especially, D2 play crucial roles in forming the μ-CTX receptor. Charge-neutralizing mutations in D1 and D2 (Asp^{384}, Asp^{762}, and Glu^{765}) had no effect on toxin binding. However, mutations at a neutral and an anionic site (residues 728 and 730) in S5-S6/D2 of rSkM1, which are not in the putative pore region, were found to decrease significantly the μ-CTX affinity with little effect on tetrodotoxin binding (≤1.3-fold increase in affinity). Furthermore, substitution at Asp^{730} with cysteine and exposure to Cd^{2+} or methanethiosulfonate reagents had no significant effect on sodium currents, consistent with this residue not contributing to the pore.

INTRODUCTION

Different toxins extracted and purified from many animal species have been useful tools to probe the molecular structure of voltage-gated ion channels. The binding of toxin to the extracellular surface of the intrinsic membrane protein results in changes in channel electrophysiological properties that interfere with normal cell excitability leading to paralysis (Catterall, 1992; Ellinor et al., 1994; Kallen et al., 1993; Miller, 1995). Natural toxins were first used to distinguish between Na^+, K^+, and Ca^{2+} currents recorded under voltage clamp conditions and, subsequently, to identify channel isoforms within a given ion-specific channel family. They have also proven useful in the purification of voltage-dependent channels and in probing the tertiary structure of their binding sites.

The small 22-amino-acid peptide μ-conotoxin GIIIA (net charge, +6) (Cruz et al., 1985; Sato et al., 1991) isolated from the piscovorous gastropod marine snail *Conus geographus* was shown to reduce the peak current amplitude of rat skeletal muscle and eel electroplax sodium channel isoforms (Chen et al., 1992; Cruz et al., 1985; Ohizumi et al., 1986; Trimmer et al., 1989; Yanagawa et al., 1987). The isoform-discriminatory ability of this toxin is high as neither brain (Moczydlowski et al., 1986) nor heart isoforms show high-affinity μ-conotoxin (μ-CTX) binding (Chahine et al., 1995; Chen et al., 1992; Gellens et al., 1992; White et al., 1991). μ-CTX binding is competitive with that of the guanidinium toxins, tetrodotoxin (TTX) and saxitoxin (STX), leading to their classification within the same toxin receptor site grouping, i.e., class 1 (Catterall, 1992).

The three-dimensional structure of μ-CTX has been elucidated (Lancelin et al., 1991), and it is a relatively rigid, compact molecule by virtue of the presence of three disulfide bridges (Hidaka et al., 1990). Each of the positively charged amino acids of μ-CTX is located at the periphery of the molecule. One (Arg13) has been shown to be particularly crucial for binding to sodium channels (Becker et al., 1992; Chahine et al., 1995; Sato et al., 1991) and extends toward or into the pore restricting ion flow (French et al., 1996).

Received for publication 27 January 1998 and in final form 30 March 1998.

Abbreviations: Ch, channel; CMV, cytomegalic virus; μ-CTX, μ-conotoxin; D, domain; ID, interdomain; I_{Na}, sodium current; hH1, human heart voltage-gated sodium channel isoform 1; MTS, methanethiosulfonate; MTSET, [2-(trimethylammonium)ethyl]methanethiosulfonate; S, transmembrane segment; rSkM1, rat skeletal muscle sodium channel isoform 1 (also named μ_1); T, toxin; TTX, tetrodotoxin; WT, wild-type.

Amino acids are designated by single- or triple-letter codes. The notation for a mutation is X#B (where X is WT and B is the replacement amino acid and # is the site in the amino acid sequence). Each of multiple mutations present in the same protein are separated by forward slashes (i.e., X#B/Z#U is a double mutation). For clarity, channel sequence numbers are superscripted (e.g., Asp^{730}) whereas toxin residues are not (e.g., Arg13). Chimera domains are designated S or H depending upon whether they originate from rSkM1 or hH1; the prime notation indicates that a major portion but not all of the domain is S or H (Fig. 2).

Address reprint requests to Dr. M. Chahine, Laval Hospital, Research Center, 2725, Chemin Ste.-Foy, Ste.-Foy, Québec, Canada G1V 4G5. Tel: 418-656-8711, ext. 5447; Fax: 418-656-4509; E-mail: mohamed.chahine@ phc.ulaval.ca.

0006-3495/98/07/236/11 $2.00

The rigidity of μ-CTX makes this toxin an ideal candidate to serve as a molecular caliper to deduce the architecture of the sodium channel outer vestibule, a necessity for understanding the mechanism of ion channel function and for rational drug design (Chahine et al., 1995; Goldstein et al., 1994). The determination of pairwise interactions between specific channel and toxin residues has been fruitful in establishing the outer vestibule architecture of voltage-gated potassium channels (Miller, 1995). For sodium channels such studies promise, in addition, to reveal the domain arrangement in three dimensions. This indirect approach to structure determination is mandated by the fact that there remain, at present, major difficulties in applying NMR or crystallographic approaches to large, nonabundant membrane proteins such as sodium channels.

Earlier, we used chimeras between a toxin-sensitive channel from rSkM1 and a toxin-resistant isoform from rat skeletal muscle (rSkM2) to demonstrate that more than a single domain of rSkM1 interacts with μ-CTX (Chen et al., 1992). Efforts to define the toxin (μ-CTX, TTX, and STX) binding regions of sodium channels have also involved site-specific mutations (Backx et al., 1992; Chen et al., 1992; Noda et al., 1989; Satin et al., 1992; Stühmer et al., 1989; Terlau et al., 1991). Many point mutations in TTX-sensitive channels helped to establish that the TTX/STX toxin-binding sites involve two rings of negatively charged amino acids. Some of these residues probably reside in the pore (defined as the SS1 and SS2 segments or P-region located in the S5-S6 loop) by the criterion that these mutations affect ion selectivity and/or single-channel conductance (Chen et al., 1992; Heinemann et al., 1992; Terlau et al., 1991). These results are consistent with earlier data showing that negatively charged amino acid side chains on the sodium channel are crucial for the binding of the positively charged TTX molecule as changes in the affinity of this toxin resulted from treatment of the channel with carboxyl-modifying, charge-neutralizing reagents, monovalent and divalent metal ions, and protons (Worley et al., 1986). As noted, competitive binding between TTX/STX and μ-CTX for receptor site 1 suggests that these toxins share, at least in part, the same binding site. However, most mutations that significantly affect TTX binding only slightly reduce the affinity of the much larger μ-CTX molecule for the sodium channel (Chahine et al., 1995; Chen et al., 1992; Stephan et al., 1994), indicating that although receptor sites for these toxins may overlap, the μ-CTX site must involve other unique interactions. Regarding channel residues involved with μ-CTX binding, the most significant finding to date is a 48-fold increase of $IC_{50}^{mutant}IC_{50}^{wild\text{-}type}$ ratio by replacing glutamate (negatively charged) at position 758 (P-region of D2) by a neutral glutamine, E758Q (Dudley et al., 1995). This mutation also decreases the μ-CTX association rate constant for toxin binding to the channel without affecting the dissociation rate constant, leading to the hypothesis that it may be involved in the electrostatic guidance of the toxin toward its receptor site. These data led to a structural model of class 1 toxin-binding sites on the external surface of the sodium channel pore (Lipkind et al., 1994) that has recently been revised (Chang et al., 1997).

In this paper, to obtain a better idea of where the μ-CTX binds to the channel, we applied a chimeric channel strategy (Chen et al., 1992; Ellinor et al., 1994) in which chimeras were constructed from portions of two channels, one donor is μ-CTX-sensitive rSkM1 and the other is μ-CTX-resistant hH1. The human skeletal muscle sodium channel isoform cannot profitably be used for chimera formation as it, unexpectedly, is relatively resistant to μ-CTX (Chahine et al., 1994). Studies of the chimeras described herein have implicated primarily D2 and to a lesser extent D1 and D4 of the channel in μ-CTX binding interactions. With a higher-resolution examination of D2 by site-directed single-amino-acid substitution analysis, we have discovered that the 728–730 region of S5-S6/D2 significantly affects μ-CTX binding, whereas mutations at these sites are associated with only a slight increase in the affinity of TTX (≤1.3-fold). These are the first mutations outside of the conventionally defined P-regions to affect the affinity of μ-CTX for rSkM1 and begin to delineate nonpore regions of the outer vestibule involved in toxin binding.

MATERIALS AND METHODS

Solutions

The Ringer's bathing solution contained (mM): 116 NaCl, 2 KCl, 1.8 $CaCl_2$, 2 $MgCl_2$, 5 HEPES; pH was adjusted to 7.6 at 22°C with NaOH. μ-CTX was obtained either from LC Laboratories (Woburn, MA) or from Sigma (Mississauga, Ontario, Canada), and TTX was purchased from Research Biochemicals International (Natick, MA). Stock solutions of toxins were made in water at 10^{-3} M and stored at −20°C.

Mutagenesis of rSkM1

Site-directed mutations were made in single-strand templates with synthetic oligonucleotides as described previously (Chen et al., 1992). pS1S1 (pSelect-1/rSkM1) has been described (Chahine et al., 1996). pS1S1′ is a cassetted version of pS1S1with *Sal*I, *Sac*I, *Hpa*1, and *Afl*II sites introduced as silent mutations at nucleotides 2171, 2843, 3967, and 4568, respectively, using the following antisense oligonucleotides: *Sal*I 5′-TACCCAGGTC-GACAAAGGGGT-3′, *Sac*I 5′-CACTGAAGGAGCTCAGCAGGA-3′, *Hpa*1 5′-CAAACAAGTTAACCCCCATGA-3′, and *Afl*II 5′-TGTCCAC-CTTAAGCTGGCTCT-3′. The underlined nucleotides are the mutation sites.

pS1H1 (pSelect-1/hH1) has been described (Chahine et al., 1996). pS1H1′ is a cassetted version of pS1H1 with *Spl*I, *Sal*I, *Sac*I, *Hpa*I, and *Afl*II, introduced as silent mutations at nucleotides 1394, 2305, 2967, 4209, and 4813, respectively, using the following antisense oligonucleotides: *Spl*I 5′-TTTGCTCCTCGTACGCCATTGCGA-3′, *Sal*I 5′-TGATGGTGAG-GTCGACAAACGGGTCCATG-3′, *Sac*I 5′-TGAAGGAGCTCAGCAG-CAAGG-3′, *Hpa*I 5′-CAAAGAGGTTAACGCCCATGA-3′, and *Afl*II 5′-GGCCAAGATGTTGATCTTAAGAGGACTTTGGTCATC-3′.

The construction of a channel chimera was described elsewhere (Frohnwieser et al., 1997). Site-specific mutation reactions not previously described (Chahine et al., 1995; Chen et al., 1992) employed the following mutagenic oligonucleotides: A728L, 5′-TTGCAGTCTGAGAGGATCTT-GCACAC-3′; D730C, 5′-GGCAGGTTGCAGCATGAGGCGATCTT-3′; D730Q, 5′-AGGCAGGTTGCATTGTGAGGCGATCTT-3′; D1221Q, 5′-CAGACCCACGTTTTGGTAGTTGACCTT-3′; D762Q/E765Q, 5′-GGCCGGCCACCT*G*CATGCATTGCCACATGGTCTCGAT-3′. All con-

structs were confirmed by sequencing the sites of mutations and the newly created junctions.

Expression in *Xenopus* oocytes

The preparation of *Xenopus* oocytes has been published (Chahine et al., 1994; Chahine et al., 1992; Gellens et al., 1992). Briefly, after being treated with 2 mg/ml collagenase for 2.5–3 h, stage V or VI oocytes were microinjected with 25–50 ng cRNA or plasmid DNA (pRcCMV/rSkM1) encoding either wild-type (WT) or mutant rSkM1. pRcCMV/rSkM1 is composed of pRcCMV (Invitrogen Corp., San Diego, CA) with *Hin*dIII and *Not*I ends containing the following fragments: SK+(*Hin*dIII to *Eco*RI of multiple cloning site (MCS))/rSkM1(*Eco*RI-bounded cDNA fragment from 351-6273 (Trimmer et al., 1989))/SK+ MCS (*Eco*RI to *Not*I). The oocytes were maintained at 18°C in a twofold diluted solution of Leibovitz's L-15 medium (Gibco, Grand Island, NY) enriched with 15 mM HEPES (pH 7.6, adjusted with NaOH), 1 mM glutamine, and 50 μg/μl gentamycin. Oocytes were used for experiments 2–3 days after injection.

Electrical recording

The macroscopic Na currents (I_{Na}) from the cRNA- or DNA-microinjected oocytes were measured using voltage-clamp techniques with two microelectrodes filled with 3 M KCl. Membrane potential was controlled by a Warner oocyte clamp (Warner Instrument Corp., Hamden, CT). A ground metal shield was inserted between the two microelectrodes to minimize electrode coupling and speed the clamp rise time. The total volume of the bath was 400 μl. Bathing solution exchanges were complete in <5 s. Voltage commands were generated by computer using pCLAMP software version 5.5 (Axon Instruments, Foster City, CA). Currents were filtered at 2 kHz (-3 dB; 4-pole Bessel filter).

In the presence of TTX or μ-CTX, the reduction of current amplitude from a depolarization to a test voltage of -10 mV from a holding potential of -120 mV was defined as the fraction of block, F_B. Under the assumption that a single molecule of toxin blocks a single voltage-gated sodium channel (Cruz et al., 1985; Moczydlowski et al., 1986), the blocking constant IC_{50} (toxin concentration at which 50% of the channels are blocked) is given by $[\mu\text{-CTX}](1 - F_B)/F_B$. The kinetics of the sodium channel blockade by μ-CTX and block reversal upon washout are well described by single-exponential functions (Chahine et al., 1994; Cruz et al., 1985). The equilibrium between toxin-bound and toxin-unbound channel is defined by two processes. First, the association rate constant k_{on} is toxin-concentration dependent and defined by the formula $(1/\tau_{on} - 1/\tau_{off})/[\mu\text{-CTX}]$ where τ_{on} and τ_{off} are the time constants of toxin binding and unbinding, respectively, and are obtained from the single-exponential functions describing the time course of the binding and unbinding reactions. The dissociation rate constant k_{off} is τ_{off}^{-1}. A confirmation of the IC_{50} value is given by the dissociation constant, $K_d = k_{off}/k_{on}$. Data are expressed as mean ± SEM.

Studies with sulfhydryl reagents

Channels were treated with methanethiolsulfonate (MTS) derivatives containing an ethylsulfonate (MTSET) side chain (Toronto Research Chemical Co., Toronto, Ontario, Canada) or with Cd^{2+} at concentrations of 1 mM.

RESULTS

rSkM1 and hH1 have different sensitivities to μ-CTX

Different channel isoforms show differential sensitivities to individual members of the guanidinium (class 1) toxin group, which bind to the outer vestibule of sodium channels to block ion flow through the pore. rSkM1 currents are sensitive to both TTX and μ-CTX in the nanomolar concentration range, whereas those of hH1 are relatively resistant to both toxins with IC_{50} values > 1 μM. hSkM1, in contrast, is TTX sensitive but μ-CTX resistant; $IC_{50} = 1.2$ μM (Chahine et al., 1994). In addition to variations between isoforms, mutations in a single channel protein can also modify the relative binding affinity of various representatives of this class of toxins. Extensive observations have been made on the rat heart isoform, rSkM2 (rH1), where reversal of the homologous amino acids, tyrosine (Y401C) in rSkM1 (μ1) and cysteine (C374Y) in rSkM2 caused a switch in the relative TTX and μ-CTX sensitivities of these two isoforms (Chen et al., 1992; Satin et al., 1992; Backx et al., 1992). However, the relative change in TTX sensitivity was ~11-fold greater than that of μ-CTX with rSkM1/Y401C mutation (43.0/3.9 = 11.0):

$$1500\ \text{nM}^{IC_{50}\text{TTX(rSkM1/Y401C)}}/34.9\ \text{nM}^{IC_{50}\text{TTX (rSkM1)}} = 43.0$$

$$197\ \text{nM}^{IC_{50}\mu\text{-CTX (rSkM1/Y401C)}}/51\ \text{nM}^{IC_{50}\mu\text{-CTX(rSkM1)}} = 3.9.$$

To illustrate this point, the effects of 300 nM μ-CTX and 50 nM TTX on WT hH1 expressed in *Xenopus* oocytes is that the WT channel is relatively resistant to both TTX and μ-CTX, whereas the hH1/C373Y mutant is sensitive to 50 nM TTX but not to 300 nM μ-CTX (Fig. 1). Thus, there must be some difference in the binding sites for TTX and μ-CTX of sodium channels. Consistent with this conclusion, the reciprocal mutation rSkM2/C374Y, which converted this isoform to a channel that is more TTX and μ-CTX sensitive, also did not completely recover the sensitivity to μ-CTX found in native rSkM1 in contrast to regaining fully high TTX affinity (Chen et al., 1992). This is a further indication that these homologous residues do not play as important a role in μ-CTX binding as they do in

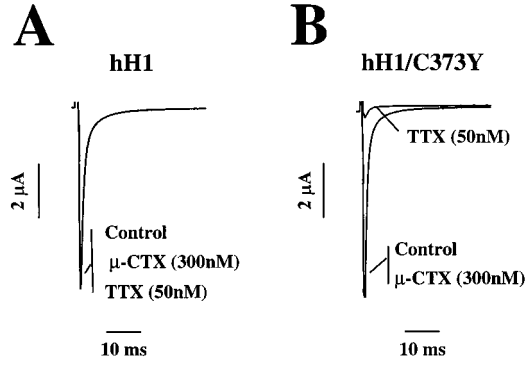

FIGURE 1 Effect of TTX and μ-CTX on wild-type and mutated hH1/C373Y sodium channels. Sodium currents were evoked by a depolarizing step from a holding potential of -120 mV to a test voltage of -10 mV from oocytes expressing (*A*) wild-type hH1 or (*B*) hH1/C373Y channels in the absence and in presence of toxins: 50 nM TTX and 300 nM μ-CTX. Neither 50 nM TTX nor 300 nM μ-CTX significantly reduced the amplitude of wild-type hH1 currents. However, TTX at 50 nM reduced dramatically sodium current from hH1/C373Y without any effect of μ-CTX at 300 nM.

TTX binding. These observations encouraged further efforts to identify the regions involved in μ-CTX binding to rSkM1 by using a chimeric channel analysis in which the chimeras are formed from two channels, one μ-CTX sensitive and one μ-CTX resistant. It was intended that this information would restrict site-specific mutagenesis experiments to portions of the channel directly involved in specifying differential toxin binding and, thus, increase the efficiency of determining the sodium channel outer vestibule architecture.

Chimeric analysis: differential μ-CTX sensitivity is determined by D1, D2, and D4

To identify which of the structural variations between hH1 and rSkM1 are responsible for the difference in the μ-CTX sensitivity, cRNA or plasmid DNA encoding WT, mutant, or chimeric sodium channels (formed from rSkM1 and hH1 isoforms, Fig. 2) were injected into *Xenopus laevis* oocytes. All of the chimeras reported herewith showed expression levels comparable to that seen with WT rSkM1 and hH1 sodium channels. The concentration dependence of the extent and rate of μ-CTX-induced current decrease (or increase after toxin washout) was measured to provide the equilibrium and rate constants for toxin association and dissociation (Fig. 2).

The chimeras are designated by four letters indicating the parent channel making the major contribution to each of the four domains. For example, SSHH is constructed with D1 and D2 from rSkM1 and D3 and D4 from hH1 (Frohnwieser et al., 1997). The origin of the NH_2 and COOH termini is the same as the adjacent domain in all cases. The affinity of μ-CTX for SSHH, $IC_{50} = 10.3 \pm 1.6$ nM ($n = 3$; Fig. 2 *C*), was increased approximately fivefold compared with that for rSkM1 (Fig. 2 *A*) ($IC_{50} = 51.4 \pm 2.2$ nM) (Chahine et al., 1995). The association rate constant was augmented 1.4-fold ($k_{on}^{SSHH} = 71.7 \pm 4.4 \times 10^3$ M^{-1} s^{-1}) for this chimera, compared with $k_{on}^{rSkM1} = 49.9 \times 10^3 \pm 10.6$ M^{-1} s^{-1} for rSkM1 (Fig. 2 *C*). The magnitude of the dissociation rate constant, $k_{off}^{SSHH} = 0.62 \pm 0.03 \times 10^{-3}$ s^{-1}, is approximately fourfold smaller for SSHH than that for rSkM1 ($2.40 \times 10^{-3} \pm 0.45$ s^{-1}; Fig. 2 *C* and Table 1). The calculated $K_d = k_{off}/k_{on}$ value of 8.7 ± 0.8 nM for SSHH agrees reasonably with the measured IC_{50} value, as was the case for all the measurements reported herein for mutant channels, but is smaller than the K_d value for rSkM1 itself due primarily to the fourfold reduction of k_{off}. To explore the basis for the increased toxin affinity of SSHH further, we examined SSHS, a chimera in which D3 derives from hH1 in a rSkM1 background (Fig. 2 *D*). The affinity and kinetic values for the μ-CTX binding reaction with this chimera, SSHS (Fig. 2 *D*), were comparable to those measured for rSkM1 (Table 1): $k_{on}^{SSHS} = 45.3 \pm 4.6 \times 10^3$ M^{-1} s^{-1} (cf. 49.9×10^3 M^{-1} s^{-1}); $k_{off}^{SSHS} = 3.1 \pm 0.5 \times 10^{-3}$ s^{-1} (cf. 2.4×10^{-3} s^{-1}); $K_d^{SSHS} = 70.8 \pm 13.4$ nM. The K_d value for the reaction of SSHS with μ-CTX agrees reasonably with the IC_{50} value of 61.5 ± 2.1 nM. Comparison of the data for SSHH and SSHS suggests that D4 from the μ-CTX-resistant heart channel contributes a greater number of positive or fewer negative interactions with the toxin than does D4 of rSkM1, although it is the latter channel that is high affinity overall. This is corroborated by parallel studies of SSSH, a chimera also exhibiting higher affinity for μ-CTX than the rSkM1 channel (Fig. 2 *E* and Table 1). The bulk of this effect is again attributable to the approximately fourfold smaller value of k_{off} for the chimera relative to that for rSkM1.

From a comparison of toxin binding between the chimeric channel SSHS and WT channel rSkM1, we have obtained evidence that there is no detectable effect of exchanging D3 (Table 1). To investigate the roles of D1 and D2 in the binding of μ-CTX, we constructed two chimeras between rSkM1 and hH1: HSSS contains D1 from hH1 and SHSS includes most of D2 from hH1 in a largely rSkM1 background (Fig. 2, *F* and *H*). The affinity of the μ-CTX for HSSS was decreased almost 22-fold ($IC_{50} = 1145 \pm 122$ nM) compared with rSkM1 ($IC_{50} = 51.4 \pm 2.2$ nM). Toxin association and dissociation rate constants were increased 2- and 21-fold, respectively: $k_{on}^{HSSS} = 109 \pm 30 \times 10^3$ M^{-1} s^{-1} (cf. 49.9×10^3 M^{-1} s^{-1}); $k_{off}^{HSSS} = 49.7 \pm 6.7 \times 10^{-3}$ s^{-1} (cf. 2.4×10^{-3} s^{-1}) (Fig. 2 *E* and Table 1); $K_d = 628 \pm 118$ nM (cf. 48.1 nM). Note that as the affinity for toxin decreases there is a trade-off between the use of higher concentrations of the costly toxin and the extent of saturation used to determine the IC_{50} values. Therefore, the agreement between calculated K_d and measured IC_{50} values tends to be less good with the lower-affinity toxins. The bulk of the decreased affinity, nevertheless, is still ascribable to much larger k_{off} values for the chimeric channel. The affinity of μ-CTX for the SHSS chimera was not measurable (current block of <3% at 300 nM μ-CTX), and a lower limit for the IC_{50} value was placed at 10 μM (Fig. 2 *H* and Table 1).

As the affinity of μ-CTX is decreased when D1 derives from hH1 and is increased when D4 is from hH1, we tested the μ-CTX sensitivity of HSSH (in which D2 and D3 originate from rSkM1 in a hH1 background) (Fig. 2 *G*). Study of this construct should enable the assessment of the relative importance of D1 and D4 in the μ-CTX binding. The μ-CTX affinity ($IC_{50} = 683 \pm 73$ nM) for this chimera is intermediate between that for SSSH and HSSS (Fig. 2). The kinetic values for HSSH were closer to those for HSSS than those for SSSH (Fig. 2 *G*), consistent with a relatively greater importance of D1 than D4 for differential toxin binding (Table 1).

Many charge-altering amino acid substitution mutations in the nonpore regions of S5-S6 loops of rSkM1 have little effect on μ-CTX affinity, with the one exception of D730

The aligned amino acid sequences of the ID5–6/D2 loop rSkM1 and hH1 show the putative S5-S6 loops of each of

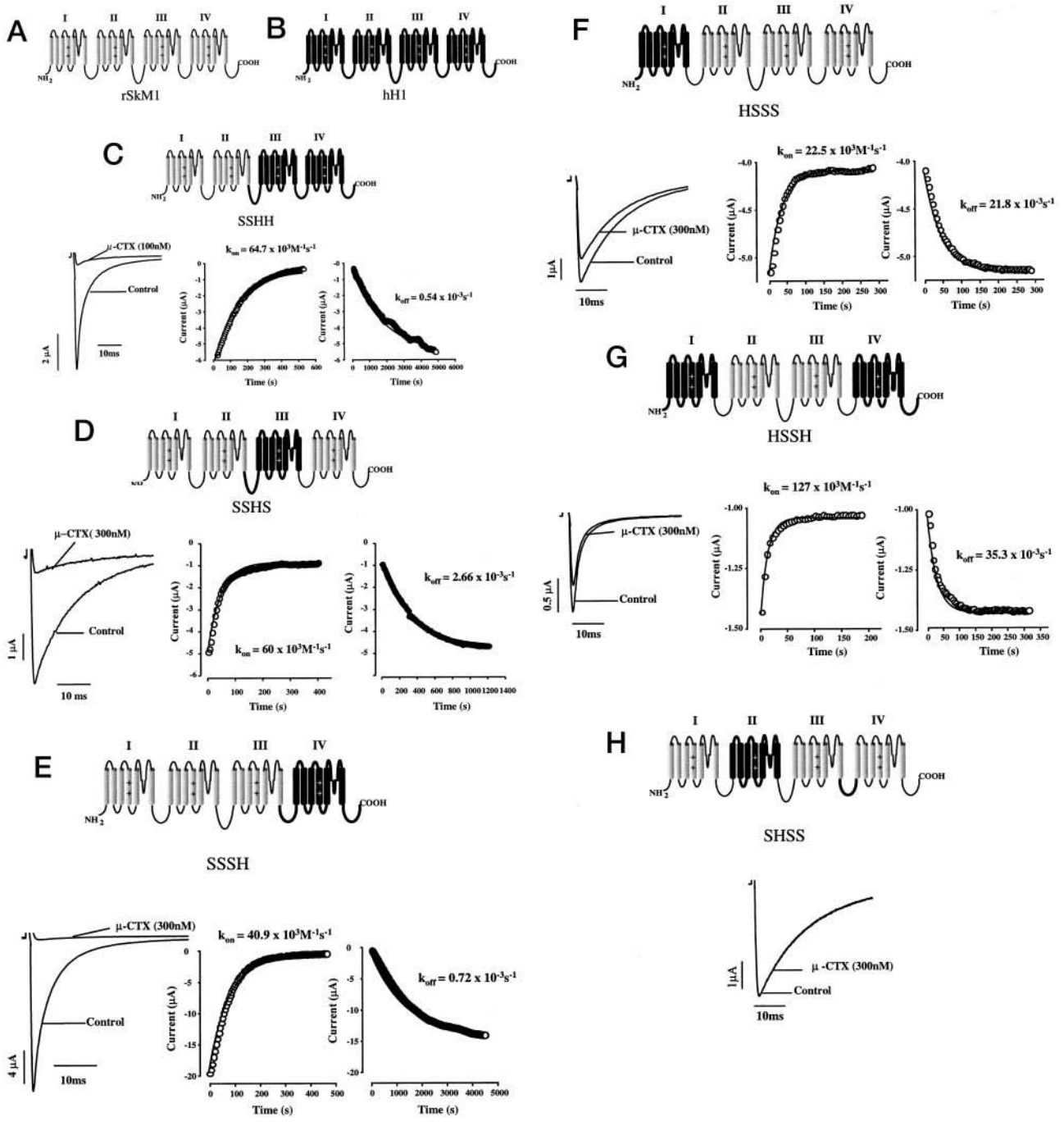

FIGURE 2 Kinetics of μ-CTX association and dissociation with chimeric sodium channels constructed from hH1 and rSkM1. Sodium currents were elicited from a holding potential of −120 mV to a test potential of −10 mV. μ-CTX was used at 100 nM (for SSHH) or 300 nM (other chimeric channels). A schematic representation of the chimeras illustrating the origin of rSkM1 (S) or hH1 (H) of the four domains is shown on the top. Below each chimera are graphs of the equilibrium block (left), kinetics of onset of block (middle), and kinetics of reversal of block (right). The solid lines are best-fit exponentials with averaged values contained in Table 1. The k_{on} and k_{off} of each experiment is also indicated. (*A*) WT-rSkM1; (*B*) WT-hH1; (*C*) SSHH; (*D*) SSHS; (*E*) SSSH; (*F*) HSSS; (*G*) HSSH; (*H*) SHSS.

the domains in Fig. 3, where single and double underlining represent SS1 and SS2 segments, respectively, containing the pore residues (Perez-Garcia et al., 1996; Li et al., 1997; Tsushima et al., 1997), the double dagger denotes possible glycosylation sites, and amino acid substitutions are placed above the site in WT rSkM1 (with replacement by glutamine (Gln or Q) generally constituting charge-neutralizing and substitution by arginine (Arg or R) being charge-introducing mutations, respectively), and asterisks indicate sites involved in multiple mutations (see Table 2 and Chahine et al., 1995). Our attempts to localize the binding site of μ-CTX by site-specific mutation at candidate anionic amino

TABLE 1 Constants for the reaction of μ-CTX with wild-type and chimeric sodium channels

Chimera	*n*	k_{on} (10^3 M^{-1} s^{-1})	Ratio	k_{off} (10^{-3} s^{-1})	Ratio	K_d (nM)	Ratio	IC_{50} (nM)	Ratio
SSSS/rSkM1*	3	49.9 ± 10.6	1.0	2.4 ± 0.5	1.0	98 ± 26	1.0	51.4 ± 2.2	1.0
SSHH	4	71.7 ± 4.4	1.44	0.62 ± 0.03	0.26	8.7 ± 0.8	0.18	10.3 ± 1.6	0.20
SSHS	3	45.3 ± 4.6	0.91	3.1 ± 0.5	1.29	70.8 ± 13.4	1.41	61.5 ± 2.09	1.20
SSSH	4	37.9 ± 4.7	0.76	0.68 ± 0.12	0.28	18.3 ± 2.0	0.37	12.8 ± 2.0	0.25
HSSS	6	109 ± 30	2.18	49.7 ± 6.7	20.7	628 ± 118	13.1	1145 ± 121	22.3
SHSS	3							>10,000	>195
HSSH	7	97.5 ± 21.9	1.95	44.9 ± 3.4	18.7	631 ± 152	13.1	683 ± 73	13.3
HHHH/hH1#								5700 ± 800	111

n = number of oocytes tested; ratio = (chimera or hH1)/WT; $K_d = k_{off}/k_{on}$. SSHH = LQ19; SSHS = LQ18; HSSS = LQ4; SHSS = LQ28; HSSH = LQ5 (Frohnwieser et al., 1997).
*Chahine et al., 1995.
#Gellens et al., 1992.

acid positions (Chahine et al., 1995) have been less successful than experiments with TTX (Terlau et al., 1991) perhaps because the larger μ-CTX molecule has more extensive binding interactions with each rSkM1 residue making a smaller contribution to the overall stability of the binary complex (see below). However, the D730Q mutation does decrease the affinity for μ-CTX (IC_{50} = 239 ± 17 nM; Table 2). The association and dissociation rate constants were increased 3.3- and 13.2-fold respectively: k_{on} = 164.6 ± 32 × 10^3 M^{-1} s^{-1} and k_{off} = 31.72 ± 5 × 10^{-3} s^{-1} (Fig. 4, *B* and *C*) and the K_d value (220.3 ± 46.5 nM) is increased relative to that of rSkM1, primarily due to the augmented k_{off} value. The failure to date of anionic charge-neutralizing mutations, other than E758Q (Dudley et al., 1995) and D730Q or D730C (this work), on the putative extracellular surface or outer vestibule of rSkM1 (i.e., S5-S6

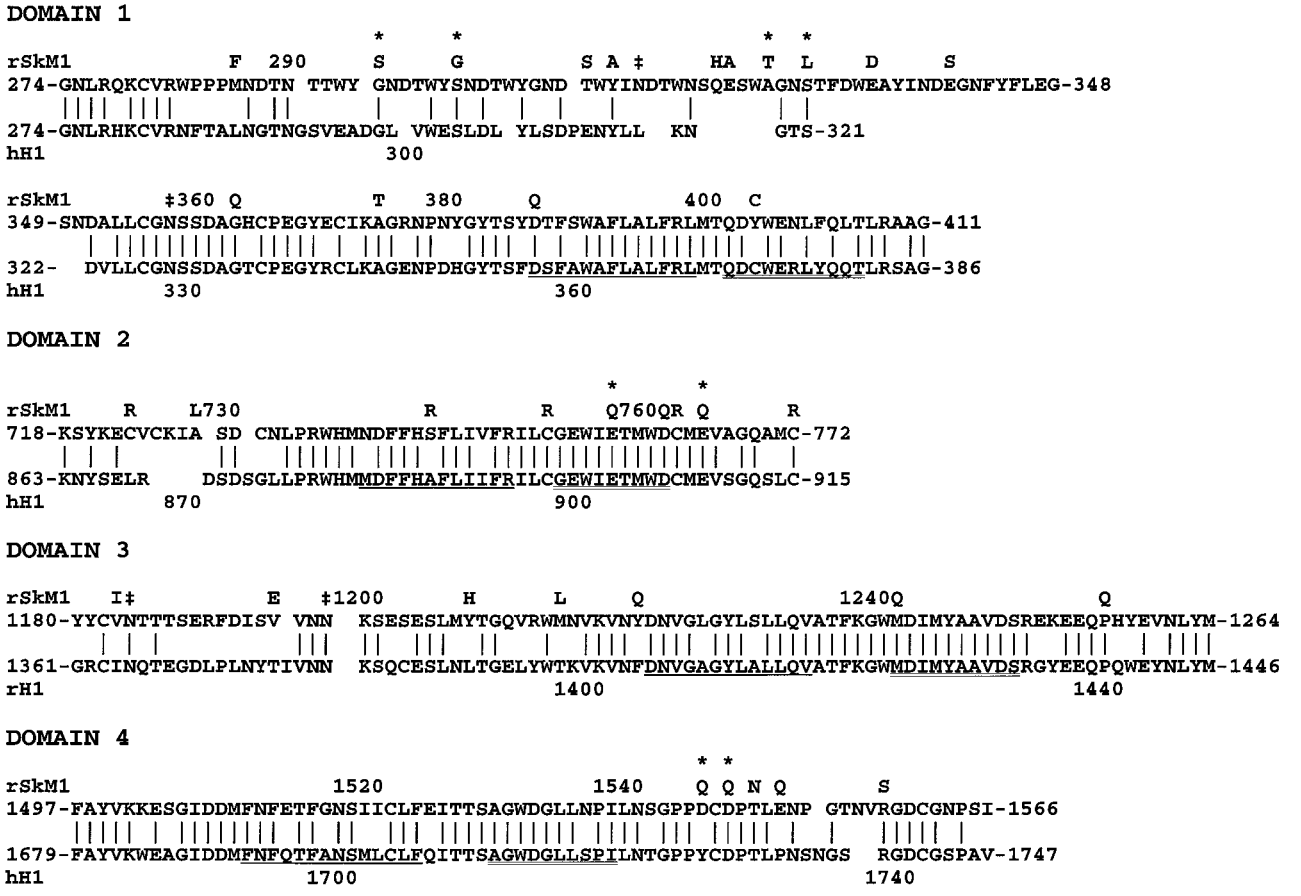

FIGURE 3 Alignment of amino acid sequences of S5-S6 loops of rSkM1 and hH1 D1-D4. Single and double underlining represent SS1 and SS2 segments, respectively, ‡Possible glycosylation sites; amino acid substitutions are placed above the mutated areas (Q generally being a charge-neutralizing and R a charge-introducing mutation). *Site of multiple mutations (see Table 2 and Chahine et al., 1995).

TABLE 2 Constants for the reaction of μ-CTX with rSkM1 site-specifically mutated sodium channels

Mutant	n	k_{on} (10^3 M^{-1} s^{-1})	Ratio	k_{off} (10^{-3} s^{-1})	Ratio	K_d (nM)	Ratio	IC_{50} (nM)	Ratio
WT*	3	49.9 ± 10.6	1.0	2.40 ± 0.45	1.0	98 ± 26	1.0	51.4 ± 2.2	1.0
D384Q	3							63.8 ± 7.3	1.24
A728L	3	325 ± 62	6.5	85.3 ± 3	35.5	245.6 ± 98.3	2.5	289 ± 62	5.6
D730Q	4	164.6 ± 32	3.3	31.72 ± 5	13.2	220.3 ± 46	2.2	239 ± 17	4.6
D762Q/E765Q	3							41.8 ± 6.9	0.81
D1221Q	3							33.1 ± 1.0	0.64

n = number of oocytes tested; ratio = mutant/WT; $K_d = k_{off}/k_{on}$.
*See also Chahine et al., 1995.

loops) to affect the μ-CTX binding energy suggests that if multiple electrostatic interactions at several different specific side chains are important, there must be other sites that remain to be identified. At present we can rule out the involvement of the following rSkM1 anionic sites in μ-CTX binding: D^{384}, D^{762}, E^{765}, D^{1221}, E^{1251}, D^{1376}, E^{1513}, E^{1524}, and E^{1555} (Table 2 and Chahine et al., 1995).

We pursued a charge-introduction approach in which arginine-scanning mutagenesis was used to attempt to delineate the footprint of the μ-CTX-channel interaction surface. It was expected that the large, cationic guanidinium side chain of arginine, if placed close to or within the toxin footprint, would interfere with toxin binding. However, of five such mutations in the S5-S6 loop of D2 (Fig. 3), only rSkM1/C725R expressed, and in that case at such low levels that toxin binding studies were not possible. Three of the other four mutations were in the P-region and may have disrupted proper channel folding, stability, or membrane insertion, or these mutations may alter the conductance in such a way that will enable us to measure sodium currents.

Residues at positions 728 and 730 of the S5-S6 loop of domain 2 of rSkM1 affect μ-CTX affinity more than that of TTX

When the alanine at position 728 of rSkM1 was mutated to leucine, the affinity of the μ-CTX for this mutant channel was reduced (IC_{50} = 289 ± 62 nM) (Fig. 5). The association and dissociation rate constants were increased 6.5- and 35.5-fold, respectively: $k_{on} = 325 \pm 44 \times 10^3$ M^{-1} s^{-1} and $k_{off} = 85.3 \pm 3 \times 10^{-3}$ s^{-1} (Fig. 4, *B* and *C*) and the K_d value (245.6 ± 98.3 nM) is increased relative to that of rSkM1, primarily due to the augmented k_{off} value. This finding provides additional evidence for the importance of this region of the channel for toxin binding, consistent with the approximately fivefold decrease in toxin affinity seen for the D730Q mutation noted above. We have noted earlier the noncorrespondence of the effects of many mutations on TTX versus μ-CTX binding. This is true for the rSkM1/A728L mutation as well. The affinity of TTX for the A728L channel (IC_{50} = 22 ± 2 nM) is 1.3-fold greater than that for the WT rSkM1 (IC_{50} = 29 ± 1 nM) (Fig. 6).

Does the 728–730 region of rSkM1 contribute to the pore structure?

To probe the possibility that this region actually contributes to the P-region itself, we used the reaction of MTSET, a methanethiosulfonate reagent containing a trimethylammonium ethyl side chain, and Cd^{2+} with D730C, being the closest residue to the DII(SS1) region of the segment studied. The purpose of this study was to investigate whether permeation properties were altered in the chemically reacted

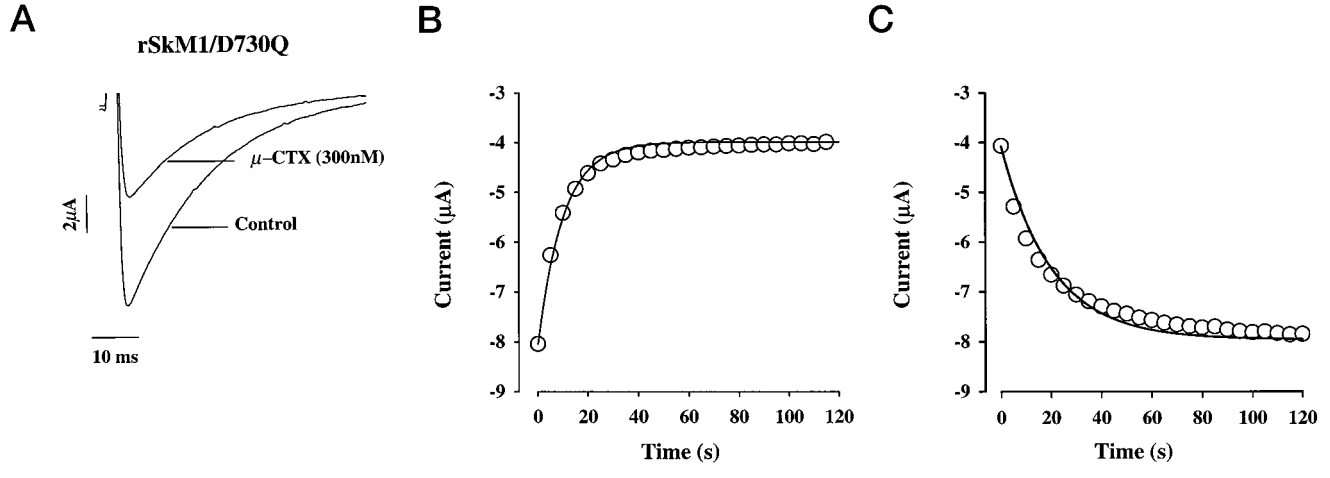

FIGURE 4 Effects of μ-CTX on rSkM1/D730Q and kinetics of μ-CTX association and dissociation. Sodium currents were elicited from holding potential of −120 mV to a test potential of −10 mV from oocytes expressing rSkM1/D730Q. (*A*) Sodium current block at equilibrium by 300 nM μ-CTX; (*B*) kinetics of onset of block; (*C*) kinetics of reversal of block by washout of toxin. The solid lines are best-fit exponentials with averaged values contained in Table 2.

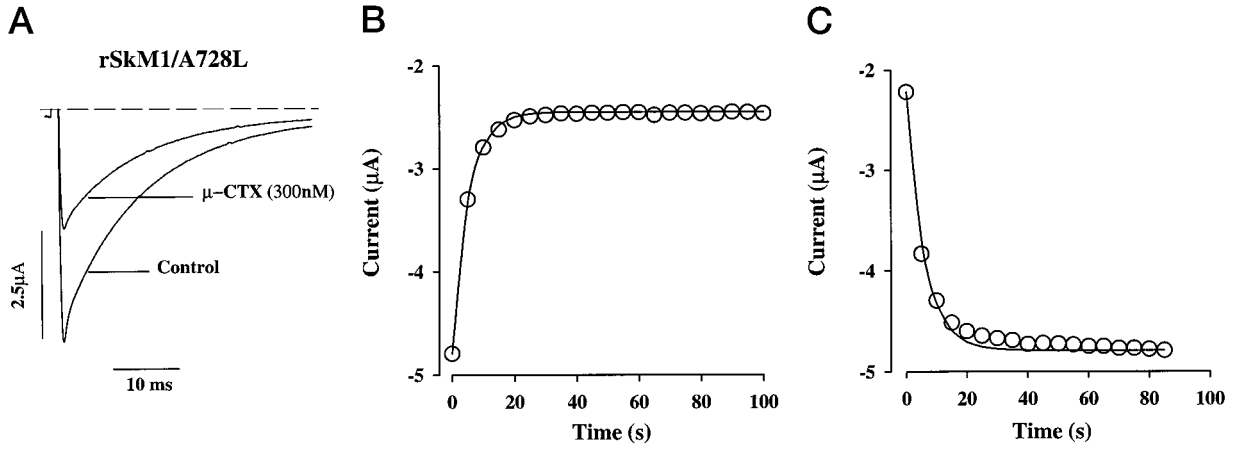

FIGURE 5 Effects of μ-CTX on rSkM1/A728L and kinetics of μ-CTX association and dissociation. Sodium currents were elicited from a holding potential of −120 mV to a test potential of −10 mV from oocytes expressing rSkM1/A728L. (*A*) Sodium current block at equilibrium by 300 nM μ-CTX; (*B*) kinetics of onset of block; (*C*) kinetics of reversal of block by washout of toxin. The solid lines are best-fit exponentials with averaged values contained in Table 2.

mutant channel relative to that of WT (Fig. 7). For rSkM1 and rSkM1/D730C, 1 mM Cd^{2+} decreases, respectively, 12 ± 0.6% (n = 4) and 14.7 ± 1.3% (n = 4) of the amplitude of sodium currents, whereas on hH1 more than 95% of the block was recorded. In the presence of MTSET we recorded less than 1% of the block for rSkM1 and rSkM1/D730C, whereas on hH1 a 13.6 ± 1.4% (n = 4) reduction of the amplitude of the current was obtained. Furthermore, the effect of μ-CTX on D730C was comparable to the one observed with D730Q (data not shown). These data suggest that the substantial effects on toxin binding exerted by the A^{728} and D^{730} segment are not due to contributions of this region to the structure of the pore itself.

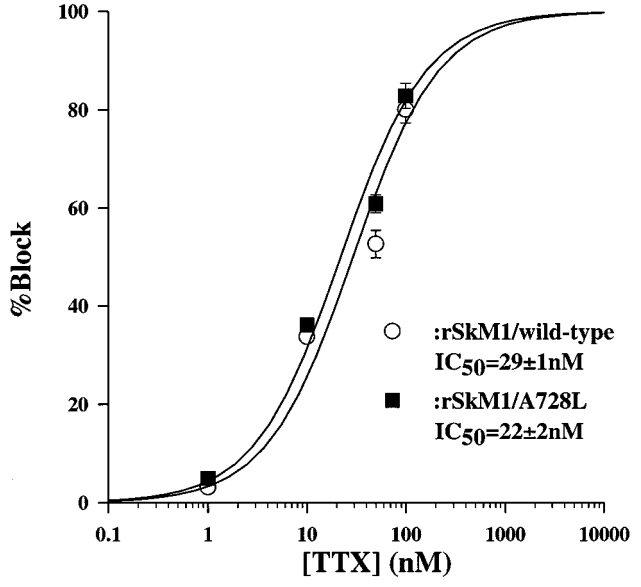

FIGURE 6 Dose-response curve of the effects of TTX on WT-rSkM1 and on rSkM1/A728L currents. The dose-response curve (mean ± SEM) for TTX block of sodium currents in five oocytes is shown. The theoretical curves are the best fits to a one-site model of block with indicated IC_{50}. See Materials and Methods for calculation of IC_{50} values.

DISCUSSION

There are a number of strategies to determine the sites at which mutations can be made: 1) predictions of the forces involved based on the known structure of the toxin (e.g., electrostatic interactions), 2) examination of sites known to be important for binding other class 1 toxins, that is, by analogy, 3) identification of side chains that, when derivatized, alter toxin binding (e.g., carboxylate reagents), and 4) searches for nonhomologous segments or sites between channel isoforms based on the assumption that differences in toxin binding must reflect differences in primary sequence between the channel proteins. In this communication, we have used the first and last approaches. Thus, before making a large investment of resources in the construction and study of point mutations at sites on the external surface of the channel, we chose to identify first the individual domains of the channel that make the greatest contributions to the high-affinity binding of the rSkM1 channel for toxin by using chimeric channels composed of various domains from rSkM1 (μ-CTX sensitive) and hH1 (μ-CTX resistant) channels (Chen et al., 1992).

Which channel domains are involved in high-affinity μ-CTX binding?

From the differences in toxin binding to this panel of chimeric channels, we have obtained evidence that the order of influence for high-affinity binding is D2 > D1 > D4 with no detectable effect of exchanging D3 (Table 1). This does not mean that D3 does not contribute to toxin binding but rather that it contributes comparably whether the source of this segment is rSkM1 or hH1. Surprisingly, as hH1 is a

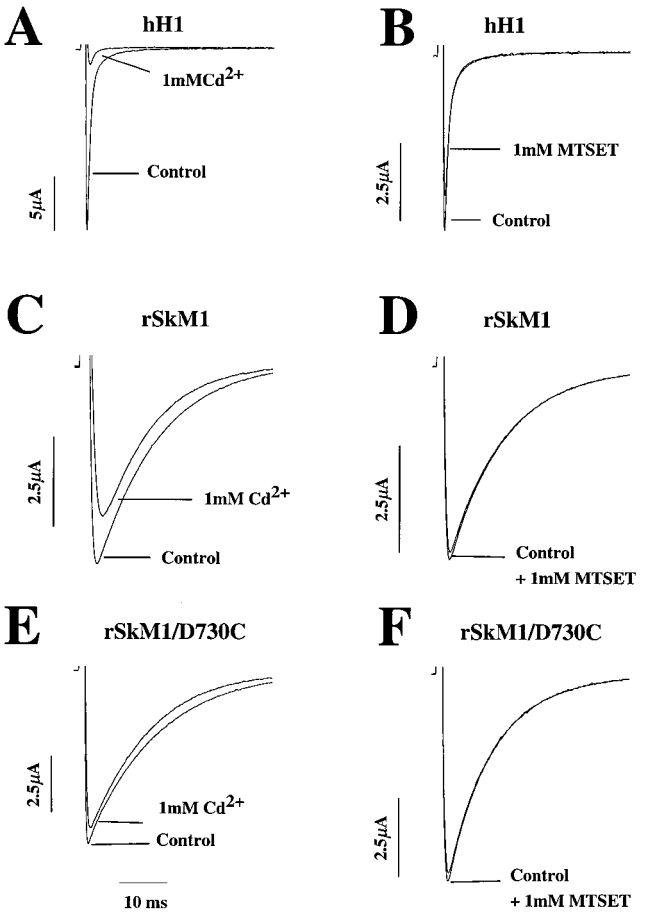

FIGURE 7 Effects of cadmium and MTSET on wild-type hH1 and rSkM1 and rSkM1/D730C sodium channels. (*A* and *B*) hH1; (*C* and *D*) rSkM1; (*E* and *F*) rSkM1/D730C mutant sodium channels. Sodium currents were recorded from a holding potential of −120 mV to −10 mV test potential. (*A*) Application of 1 mM cadmium significantly reduces the amplitude of sodium current from hH1 but has a only a small effect on rSkM1 (*C*) and rSkM1/D730C mutant sodium channels (*E*). Exposure to 1 mM MTSET reduces the sodium current by ~20% with hH1 (*B*) and has even smaller effects on the amplitude of rSkM1 and rSkM1/D730C mutant sodium channels (*D* and *F*).

μ-CTX-resistant channel, we have identified D4/hH1 as conferring increased affinity for μ-CTX in chimeric channels when it replaces D4/rSkM1. Whether this is due to negative influences exerted by structural elements of D4/rSkM1 or to additional positive interactions between D4/hH1 and toxin is a subject for future study.

Which channel amino acid residues are involved in μ-CTX binding?

The order of influence of domains on high-affinity toxin binding, resulting from the studies of chimeras, led us to focus our initial mutagenesis efforts on D2. The least conserved segment in the S5-S6/D2 loop extends from 728–732. Although there is no clear-cut segregation of residues to toxin-sensitive and -resistant phenotypes, site-specific substitutions led to the identification of A^{728} as an important interaction site (hH1 has S^{871} at the comparable position). This is the first residue of rSkM1 we have found that, when substituted, affects toxin affinity and is not located in the putative P-region. The side chain of Ala^{728} is believed to be involved in short-range interactions with toxin based on the criterion that the mutation affects k_{off} values predominantly (cf. Glu^{758} and Asp^{1532}, see below). Additional evidence that the segment around Ala^{728} is involved in toxin binding comes from studies of the A728L, D730Q, and D730C mutant channels, which show much decreased affinities for μ-CTX.

The fact that no changes in sodium currents, relative to the WT channel, were detected by exposure of rSkM1/D730C to Cd^{2+} or MTSET suggests that although this region has a substantial effect on toxin binding, it does not contribute to the pore region. The effect, then, most likely is because this region contributes to the outer vestibule and the μ-CTX binding site. Alternatively, the effect may be indirect, perhaps altering the secondary or tertiary structure of other residues in the outer vestibule that are directly in contact with the toxin when the latter is bound. The resolution between these two possibilities will require additional experiments.

Replacement of amino acid Glu^{758} (D2) by Gln has been shown to induce a 48-fold reduction of the affinity of the highly net-positively-charged μ-CTX for the channel (Dudley et al., 1995). The comparable mutation in rat brain II channels (E945Q) also produces a reduced affinity of guanidinium toxins, in this case TTX (Terlau et al., 1991). Surprisingly, most of the other amino acids that are known to affect TTX binding to rSkM1 significantly have only minor effects on the affinity of μ-CTX for the mutant channel, although the binding sites for these toxins apparently overlap as revealed by competition studies (Catterall, 1992; Chahine et al., 1994; Chen et al., 1992; Dudley et al., 1995; Stephan et al., 1994). The noncorrespondence is true for the rSkM1/A728L mutation as well. The A728L mutation has only a 1.3-fold effect on TTX affinity compared with that for the WT rSkM1 (Fig. 6).

Extending this analysis, we have also scanned the S5-S6 loops by examining charge-neutralizing mutations at anionic sites in all of the domains (Table 2) based on the reasonable assumption that electrostatic interactions may be dominant in binary complex formation with a toxin possessing a net charge +6 with radially extended cationic side chains (Lancelin et al., 1991). This rationale is supported by the importance of carboxylate side chains in guanidinium toxin binding (Cherbavaz and Miller, 1991; Dudley and Baumgarten, 1993) and by analogy to K-channel-peptide toxin interactions (Miller, 1995).

At present we can rule in roles for D^{400}, E^{403}, E^{758}, D^{1241}, and D^{1532}. In the cases of Glu^{758} and Asp^{1532}, it appears that these mutations encompass distant electrostatic effects that provide a guidance role, a conclusion based on the finding that the major effect is on k_{on} values (Penzotti et al., 1996). The large body of mutations that we have analyzed and appear to be innocuous does rule out the following sites

from being involved with the toxin-channel interaction surface: D^{384}, D^{762}, E^{765}, D^{1221}, E^{1251}, D^{1376}, E^{1513}, E^{1524}, and E^{1555} (Table 2) (Chahine et al., 1995; Dudley et al., 1995; Li et al., 1997; Penzotti et al., 1996; Stephan et al., 1994). A natural consequence of the negative results was to suspect that additional sites, including those that participate in other types of interactions (e.g., van der Waals or π-cation), must be investigated to fully understand toxin binding. We created a set of cysteine-scanning mutations through the SS2 segments of the four domains, and their effects on toxin binding, combined with sulfhydryl reagent studies, led to the identification of five P-region residues (in addition to Y^{401} and E^{758}, previously reported) that significantly affect binding of μ-CTX to Na channels (D^{400}, W^{402}, W^{1239}, D^{1241}, and W^{1531}) (Li et al., 1997). In the case of the three tryptophan residues, mutation to cysteine increases the affinity of μ-CTX, an effect that is reversible by exposure of the cysteine-substituted channels to benzylmethanethiolsulfonate (MTSBN), a reaction that restores an aromatic side chain at these sites. Clearly the Y^{401}, W^{402}, W^{1239}, and W^{1531} sites involve interactions other than electrostatic (Chahine et al., 1995; Li et al., 1997).

What is the structure of the outer vestibule?

The three-dimensional structure of μ-CTX vaguely resembles a tetragonal bipyramid with a top-to-bottom distance of ~25 Å and a diameter of ~20 Å (Lancelin et al., 1991). Based on the toxin dimensions and assuming that mutations in the rSkM1 sodium channel that affect toxin affinity indicate a direct interaction of μ-CTX with the protein side chain at the site of mutation, Asp^{400}, Tyr^{401}, Try^{402}, Glu^{403}, Ala^{728}, Asp^{730}, Glu^{758}, Try^{1239}, Asp^{1241}, and Asp^{1532} must reside within 25 Å of each other. This compares to overall dimensions of the K-channel toxin-binding vestibule, which has been estimated at 25 × 35 × 15 Å (Miller, 1995). In addition, our data show that the proximal portion (residues 728–730) of the S5-S6/D2 segment does not contribute to the structure of the pore but is involved with μ-CTX binding and, thus, forms part of the outer vestibule. Thus, the μ-CTX could be an important tool to investigate the structure of the outer vestibule of sodium channels in muscle and potentially in other tissues.

We appreciate very much the collegiality extended to us by Drs. Fozzard, French, and Backx and their associates, who have provided encouragement, shared data before publication, and participated in helpful discussions.

This study was supported by the Medical Research Council of Canada MT-12554 (M. Chahine), the Heart and Stroke Foundation of Quebec (M. Chahine), the National Institutes of Health AR41,762 (R.G. Kallen), Standard grants-in-aid from the American Heart Association (Delaware Affiliate and Florida Affiliate) (R.G. Kallen), the Muscular Dystrophy Association (R.G. Kallen), and the Research Foundation of the University of Pennsylvania. Dr. Chahine is a Research Scholar of the Heart and Stroke Foundation of Canada.

REFERENCES

Backx, P. H., D. T. Yue, J. H. Lawrence, E. Marban, and G. F. Tomaselli. 1992. Molecular localization of an ion-binding site within the pore of mammalian sodium channels. *Science.* 257:248–251.

Becker, S., E. Prusak-Sochaczewski, G. Zamponi, A. G. Beck-Sickinger, R. D. Gordon, and R. J. French. 1992. Action of derivatives of μ-conotoxin GIIIA on sodium channels. Single amino acid substitutions in the toxin separately affect association and dissociation rates. *Biochemistry.* 31:8229–8238.

Catterall, W. A. 1992. Cellular and molecular biology of voltage-gated sodium channels. *Physiol. Rev.* 72:s15–s48.

Chahine, M., P. B. Bennett, A. L. George, Jr., and R. Horn. 1994. Functional expression and properties of the human skeletal muscle sodium channel. *Pflugers Arch. Eur. J. Physiol.* 427:136–142.

Chahine, M., L. Q. Chen, R. L. Barchi, R. G. Kallen, and R. Horn. 1992. Lidocaine block of human heart sodium channels expressed in *Xenopus* oocytes. *J. Mol. Cell. Cardiol.* 24:1231–1236.

Chahine, M., L.-Q. Chen, N. Fotouhi, R. Walsky, R. Fry, R. Horn, and R. G. Kallen. 1995. Characterizing the μ-conotoxin binding site on Na Channels with analogs and point mutations. *Receptors Channels.* 3:161–174.

Chahine, M., I. Deschene, L. Q. Chen, and R. G. Kallen. 1996. Electrophysiological characteristics of cloned skeletal and cardiac muscle sodium channels. *Am. J. Physiol.* 271:H498–H506.

Chang, N. S., S. Dudley, Jr., G. Lipkind, R. J. French, and H. Fozzard. 1997. μ-Conotoxin binding to the voltage-gated Na^+ channel: structural implications for the outer vestibule. *Biophys. J.* 72:A361.

Chen, L. Q., M. Chahine, R. G. Kallen, R. L. Barchi, and R. Horn. 1992. Chimeric study of sodium channels from rat skeletal and cardiac muscle. *FEBS Lett.* 309:253–257.

Cherbavaz, D. B., and C. Miller. 1991. Trimethyloxonium modification of batrachotoxin-activated sodium channels weakens μ-conotoxin block. *Biophys. J.* 59:261A.

Cruz, L. J., W. R. Gray, B. M. Olivera, R. D. Zeikus, L. Kerr, D. Yoshikami, and E. Moczydlowski. 1985. *Conus geographus* toxins that discriminate between neuronal and muscle sodium channels. *J. Biol. Chem.* 260:9280–9288.

Dudley, S. C., Jr., and C. M. Baumgarten. 1993. Modification of cardiac sodium channels by carboxyl reagents: trimethyloxonium and water-soluble carbodiimide. *J. Gen. Physiol.* 101:651–671.

Dudley, S. C., Jr., H. Todt, G. Lipkind, and H. A. Fozzard. 1995. A μ-conotoxin-insensitive Na^+ channel mutant: possible localization of a binding site at the outer vestibule. *Biophys. J.* 69:1657–1665.

Ellinor, P. T., J. F. Zhang, W. A. Horne, and R. W. Tsien. 1994. Structural determinants of the blockade of N-type calcium channels by a peptide neurotoxin. *Nature.* 372:272–275.

French, R. J., E. Prusak-Sochaczewski, G. W. Zamponi, S. Becker, A. S. Kularatna, and R. Horn. 1996. Interactions between a pore-blocking peptide and the voltage sensor of the sodium channel: an electrostatic approach to channel geometry. *Neuron.* 16:407–413.

Frohnwieser, B., L.-Q. Chen, R. G. Kallen, and W. Schreibmayer. 1997. Modulation of human cardiac sodium channel hH1 α-subunits by cAMP-dependent protein kinase is conferred by the cytoplasmic loop interconnecting domains 1 and 2. *J. Physiol.* 491:309–318.

Gellens, M. E., A. L. George, Jr., L. Q. Chen, M. Chahine, R. Horn, R. L. Barchi, and R. G. Kallen. 1992. Primary structure and functional expression of the human cardiac tetrodotoxin-insensitive voltage-dependent sodium channel. *Proc. Natl. Acad. Sci. U.S.A.* 89:554–558.

Goldstein, S. A., D. J. Pheasant, and C. Miller. 1994. The charybdotoxin receptor of a Shaker K^+ channel: peptide and channel residues mediating molecular recognition. *Neuron.* 12:1377–1388.

Heinemann, S. H., H. Terlau, W. Stuhmer, K. Imoto, and S. Numa. 1992. Calcium channel characteristics conferred on the sodium channel by single mutations. *Nature.* 356:441–443.

Hidaka, Y., K. Sato, H. Nakamura, J. Kobayashi, Y. Ohizumi, and Y. Shimonishi. 1990. Disulfide pairings in geographutoxin I, a peptide neurotoxin from *Conus geographus*. *FEBS Lett.* 264:29–32.

Kallen, R. G., S. A. Cohen, and R. L. Barchi. 1993. Structure, function and expression of voltage-dependent sodium channels. *Mol. Neurobiol.* 7:383–428.

Lancelin, J. M., D. Kohda, S. Tate, Y. Yanagawa, T. Abe, M. Satake, and F. Inagaki. 1991. Tertiary structure of conotoxin GIIIA in aqueous solution. *Biochemistry.* 30:6908–6916.

Li, R. A., R. G. Tsushima, R. G. Kallen, and P. H. Backx. 1997. Pore residues critical for μ-CTX binding to rat skeletal muscle Na^+ channels (rSkM1) revealed by cysteine mutagenesis. *Biophys. J.* 73:1874–1884.

Lipkind, G., H. Fozzard, and S. Dudley. 1994. A structural model of the μ-conotoxin binding site in the sodium channel. *Biophys. J.* 66:A281.

Miller, C. 1995. The charybdotoxin family of K^+ channel-blocking peptides. *Neuron.* 15:5–10.

Moczydlowski, E., B. M. Olivera, W. R. Gray, and G. R. Strichartz. 1986. Discrimination of muscle and neuronal Na-channel subtypes by binding competition between saxitoxin and μ-conotoxins. *Proc. Natl. Acad. Sci. U.S.A.* 83:5321–5325.

Noda, M., H. Suzuki, S. Numa, and W. Stühmer. 1989. A single point mutation confers tetrodotoxin and saxitoxin insensitivity on the sodium channel II. *FEBS Lett.* 259:213–216.

Ohizumi, Y., S. Minoshima, M. Takahashi, A. Kajiwara, H. Nakamura, and J. Kobayashi. 1986. Geographutoxin II, a novel peptide inhibitor of Na channels of skeletal muscles and autonomic nerves. *J. Pharmacol. Exp. Ther.* 239:243–248.

Penzotti, J. L., S. C. Dudley, G. Lipkind, and H. A. Fozzard. 1996. A ring of negative charges at the Na^+ channel outer vestibule is involved in binding guanidinium-containing toxins. *Biophys. J.* 70:A319.

Perez-Garcia, M. T., N. Chiamvimonvat, E. Marban, and G. F. Tomaselli. 1996. Structure of the sodium channel pore revealed by serial cysteine mutagenesis. *Proc. Natl. Acad. Sci. U.S.A.* 93:300–304.

Satin, J., J. W. Kyle, M. Chen, R. B. Rogart, and H. A. Fozzard. 1992. The cloned cardiac Na channel α-subunit expressed in *Xenopus* oocytes show gating and blocking properties of native channels. *J. Membr. Biol.* 130:11–22.

Sato, K., Y. Ishida, K. Wakamatsu, R. Kato, H. Honda, Y. Ohizumi, H. Nakamura, M. Ohya, J.-M. Lancelin, and D. Kohda. 1991. Active site of μ-conotoxin GIIIA, a peptide blocker of muscle sodium channels. *J. Biol. Chem.* 266:16989–16991.

Stephan, M. M., J. F. Potts, and W. S. Agnew. 1994. The microI skeletal muscle sodium channel: mutation E403Q eliminates sensitivity to tetrodotoxin but not to μ-conotoxins GIIIA and GIIIB. *J. Membr. Biol.* 137:1–8.

Stühmer, W., F. Conti, H. Suzuki, X. D. Wang, M. Noda, N. Yahagi, H. Kubo, and S. Numa. 1989. Structural parts involved in activation and inactivation of the sodium channel. *Nature.* 339:597–603.

Terlau, H., S. H. Heinemann, W. Stühmer, M. Pusch, F. Conti, K. Imoto, and S. Numa. 1991. Mapping the site of block by tetrodotoxin and saxitoxin of sodium channel II. *FEBS Lett.* 293:93–96.

Trimmer, J. S., S. S. Cooperman, S. A. Tomiko, J. Y. Zhou, S. M. Crean, M. B. Boyle, R. G. Kallen, Z. H. Sheng, R. L. Barchi, and F. J. Sigworth. 1989. Primary structure and functional expression of a mammalian skeletal muscle sodium channel. *Neuron.* 3:33–49.

Tsushima, R. G., R. A. Li, and P. H. Backx. 1997. Altered ionic selectivity of the sodium-channel revealed by cysteine mutations within the pore. *J. Gen. Physiol.* 109:463–475.

White, M. M., L. Q. Chen, R. Kleinfield, R. G. Kallen, and R. L. Barchi. 1991. SkM2, a Na^+ channel cDNA clone from denervated skeletal muscle, encodes a tetrodotoxin-insensitive Na^+ channel. *Mol. Pharmacol.* 39:604–608.

Worley, J. D., R. J. French, and B. K. Krueger. 1986. Trimethyloxonium modification of single batrachotoxin-activated sodium channels in planar bilayers: changes in unit conductance and in block by saxitoxin and calcium. *J. Gen. Physiol.* 87:327–349.

Yanagawa, Y., T. Abe, and M. Satake. 1987. μ-Conotoxins share a common binding site with tetrodotoxin-saxitoxin on eel electroplax sodium channels. *J. Neurosci.* 7:1498–1502.